

Comparative Study between Direct Torque Control and Field-Oriented Control for Induction Machine used in Flywheel Energy Storage System

I. Hamzaoui¹, F. Bouchafaa² and A. Talha³

^{1,2,3}Laboratory of Instrumentation, Faculty of Electronics and Computer, University of Sciences and Technology Houari Boumediene, BP 32 El- Alia 16111, Bab-Ezzouar, Algiers, Algeria.
E-mail: hamzaoui_ihssen2000@yahoo.fr, fbouchafa@gmail.com, abtalha@gmail.com

Abstract: In this paper, we will conduct a detailed performance comparison of two techniques for control of cage induction machine (MAS): vector control in rotor flux oriented (FOC) and direct torque control (DTC) in transient and permanent. We focus on using this machine in inertial energy storage. The theoretical and simulation results are presented and discussed. Transient, the expected goal is to evaluate the method that gives the best response dynamics (speed without overshoot). Steady two control techniques are compared in terms of undulations.

Key words: Flywheel Energy Storage System, IM Direct torque control, Field-oriented Control.

1. Introduction

As part of a distributed generation from renewable energy may be considered to ensure a storage or backup for a local regulation of energy flow. Thus, the flywheel is particularly suited for producing renewable energy by requiring, in the case of wind power, storage capacity of a few minutes [2][3]. A flywheel mechanically coupled to an asynchronous electric machine, and can operate as a motor or generator and driven by a power converter as shown in Figure 1.

The asynchronous machine is chosen according to these benefits in terms of simplicity and robustness of the rotating parts [4][8]. Recent technological advances in power electronics and digital signal processing are open to researchers the voice command successful developments that meet the industrial requirements. The current orders are dominant in the industry, the Field-oriented Control (FOC), and direct torque control (DTC) [8].

However, both have some drawbacks, including sensitivity to internal and external uncertainties.

The vector control was introduced in the early 70's, and its actual applications have emerged a decade later [10]. However, it could actually be implemented and used with the advanced microelectronics. Indeed, it requires calculations transformed Park, evaluation of trigonometric functions, integrations, regulations, requiring a technology powerful enough.

The principle underlying the FOC is that the torque

and flux of the machine are controlled separately in similarity to the direct machine separately excited, where the stator currents are transformed in a rotating reference frame aligned with the rotor flux vector, or that of the stator or that the inter-iron, to produce components according to the axis d (control flow) and according to the axis q (torque control)

The direct torque and flux control (DTFC) was introduced there are more than twenty years by Takahashi and Depenbrook [6], different from the previous command FOC, the DTC is operating a direct torque and the flux produced by the asynchronous machine fed by the inverter. Its major advantages are fewer parameters of the machine used in his equations, no transformation between reference frames, no current regulators, PWM generator is not that dramatically improves the dynamic response, and without the use of mechanical sensors [5].

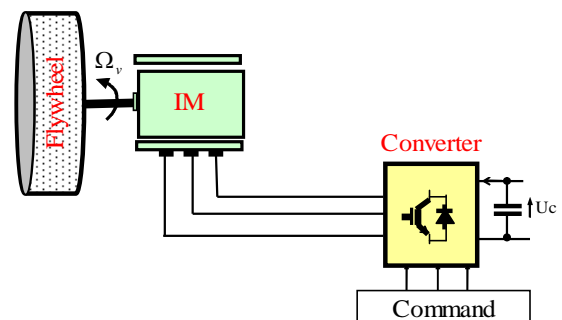


Fig. 1. Structure of the system of storage

Its main drawbacks are the limited number of available voltage vectors generates the torque ripple, flow, and steady currents that are reflected in the estimate of the speed and response, and also result in increased acoustic noise and sensitivity to variations in the stator resistance. Furthermore, deletion of the PWM stage main feature of the DTC and the introduction of hysteresis controllers for the torque and flux has the effect of having a variable switching frequency [7] [9].

In the first part of this paper, the model of the studied

system is presented, we begin by calculating the flywheel, and then we present the model of the machine in the mark Park. In the second part, two control strategies tested are presented. Finally, in the last part, the simulation results using two strategies to a reference power of the inertial energy storage are given.

2. Model of the system to study

2.1 The flywheel

The energy E_v stored in the flywheel is given by the following expression:

$$E_v = \frac{1}{2} J_v \Omega_v^2 \quad (1)$$

Where J_v is the moment of inertia of the flywheel and Ω_v its speed of rotation.

To calculate the inertia of flywheel, based on a power to be provided for a time Δt : we want the inertial storage furnish the rated power P_{masN} for a time Δt the energy required is then:

$\Delta E_v = P_{masN} \Delta t$. knowing that: $\Delta E_v = (1/2) J_v \Delta \Omega_v^2$ and that $\Delta \Omega_v^2 = \Delta \Omega_{vMAX}^2 - \Delta \Omega_{vMIN}^2$ it comes:

$$J_v = \frac{2 P_{masN} \Delta t}{(\Omega_{vMAX}^2 - \Omega_{vMIN}^2)} \quad (2)$$

According to equation (2) we find that when making a flywheel for an FESS, there are two initial conditions which must be considered: The maximum speed of rotation of the flywheel and the ability the flywheel.

The Fig. 2 represents the torque and power as a function of the speed. We notice that:

For $0 \leq \Omega_v \leq \Omega_{vN}$, the torque may be maximal giving up a power proportional to the speed $P_{IM} = K \Omega_v$.

For $\Omega_v > \Omega_{vN}$, the power is maximum and corresponds to the rated power of the machine; the electromagnetic torque is inversely proportional to the speed ($T_{em} = K / \Omega_v$).

So, if we want the machine to operate at its rated power, it is necessary to use it beyond its rated speed. Thus, we can consider that this rated speed constitutes the lower limit of the storage system and twice this speed ad the upper limit.

Thus, a field weakening operation will be necessary to obtain a constant power in the speed range of 157-314rad/s. The reference flux is then determined by:

$$\Phi_{ref} = \begin{cases} \Phi_n \Rightarrow \text{if } |\Omega| \leq \Omega_n \\ \Phi_n \frac{\Omega_n}{|\Omega|} \Rightarrow \text{if } |\Omega| > \Omega_n \end{cases} \quad (3)$$

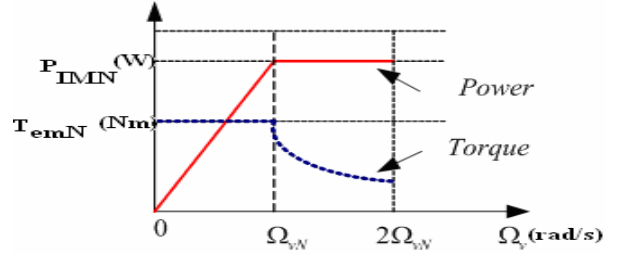


Fig. 2. Power and torque versus speed of the IM

2.2 Model of the induction machine

Under the simplifying assumptions based on an unsaturated regime without loss and distribution of the magnetic wave sinusoidal model of induction motor in Park mark is defined by the following equation:

$$\begin{cases} \sigma L_s \frac{d}{dt} i_{ds} = -R_s i_{ds} + \omega_s \sigma L_s i_{qs} - \frac{M}{L_r} \frac{d}{dt} \Phi_{dr} + \omega_s \frac{M}{L_r} \Phi_{qr} + v_{ds} \\ \sigma L_s \frac{d}{dt} i_{qs} = -R_s i_{qs} - \omega_s \sigma L_s i_{ds} - \frac{M}{L_r} \frac{d}{dt} \Phi_{qr} - \omega_s \frac{M}{L_r} \Phi_{dr} + v_{qs} \\ \frac{d}{dt} \Phi_{dr} = -\frac{R_r}{L_r} \Phi_{dr} + \omega_r \Phi_{qr} + \frac{R_r M}{L_r} i_{ds} \\ \frac{d}{dt} \Phi_{qr} = -\frac{R_r}{L_r} \Phi_{qr} - \omega_r \Phi_{dr} + \frac{R_r M}{L_r} i_{qs} \end{cases} \quad (4)$$

Where $\sigma = 1 - \frac{M^2}{L_s L_r}$ is the dispersion coefficient.

The electromagnetic torque is expressed as:

$$T_{em} = P \frac{M}{L_r} (\Phi_{dr} i_{qs} - \Phi_{qr} i_{ds}) \quad (5)$$

2.2.1 Field-oriented Control

The command of induction machine taken is a vector Control in rotor flux oriented classical: the orientation of the marker is chosen so that $\Phi_{dr} = \Phi_r$ and the flux is controlled Φ_r to keep it constant. The implementation of the command requires estimating the electromagnetic torque, the rotor flux and stator angular ω_s .

The electromagnetic torque is expressed from the current i_{qs} by:

$$T_{em} = p \frac{M}{L_r} \Phi_r i_{qs} \quad (6)$$

The rotor flux is estimated, as to him, function of the current i_{ds} and the rotor time constant $T_r = L_r / R_r$.

$$\Phi_r = \frac{M}{1 + T_r s} i_{ds} \quad (7)$$

Knowledge of ω_s ensures the validity of the equations for the repository "dq" must constantly follow the rotating field. For this, we use the angular

relationship of internal $\omega_s = \omega_r + \omega$, with $\omega = p\Omega$. The speed of rotation of the machine is measured and the rotor field is estimated. Then obtained for ω_s :

$$\omega_s = p\Omega + \frac{M i_{qs}}{T_r \Phi_r} \quad (8)$$

Starting from a reference power P_{v-ref} , we can deduce the electromagnetic torque reference of the machine, T_{em-ref} , causing the flywheel by a measure of the speed of rotation, Ω_{v-mes} .

$$T_{em-ref} = \frac{P_{v-ref}}{\Omega_{v-mes}} \quad (9)$$

The electromagnetic torque reference should be limited at nominal torque for the speed range between 0 and the rated speed, beyond the nominal speed, the torque will decrease in order to keep the product $T_{em-ref} \cdot \Omega_v$ constant. The torque reduction is carried out by the defluxing of the machine beyond the synchronous speed. The law of defluxing which has been introduced in the simulation is as follows:

$$\Phi_{dr-ref} = \frac{P_{v-ref} L_r}{p M i_{qs}} \frac{1}{\Omega_{v-mes}} \quad (10)$$

Fig. 3 shows the block diagram of the control of FESS, the currents i_{ds-ref} and i_{qs-ref} are determined by the flow regulator for the d -axis current, and the electromagnetic torque reference for the q -axis current. The electromagnetic torque being calculated from equation (9), the quadrature current is determined by inverting the torque equation (6).

2.2.2 Direct Torque Control

The direct torque control (DTC) based on the orientation of the stator flux, uses the instantaneous values of voltage vector. A three-phase inverter with two voltage levels has six switching cells giving eight possible switching states (Fig. 4). Among these eight vectors, the vector v_0 and v_7 lead to zero-voltage the terminals of the asynchronous machine; the others give, in the reference frame α - β , the six directions that can take the voltage vector. These vectors are selected from a switching table in function of errors of flow, torque and the position of the stator flux vector [1]. The vector voltage v_s can be written as:

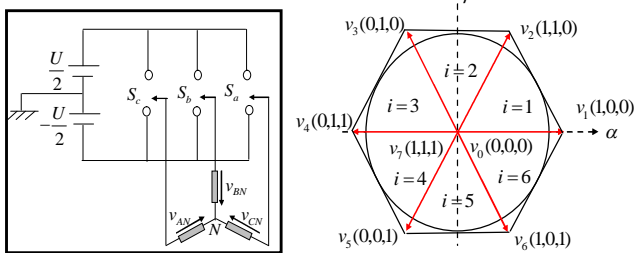


Fig. 4. Inverter and its switching vectors

Fig. 5 shows the general diagram of the DTC

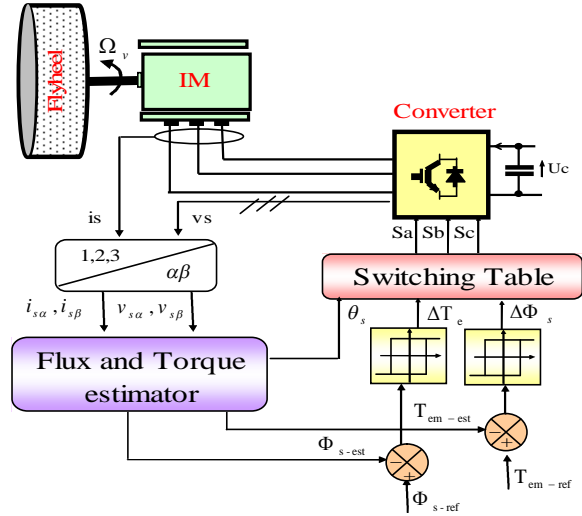


Fig. 5. Block diagram of direct torque control

$$v_s = \sqrt{2/3} U_0 [S_a + S_b e^{j2\pi/3} + S_c e^{j4\pi/3}] \quad (11)$$

The stator flux Φ_s and the electromagnetic torque T_{em} are calculated from the following equations:

$$\Phi_s = \sqrt{\Phi_{s\alpha}^2 + \Phi_{s\beta}^2} \quad (12)$$

$$\Phi_{s\alpha} = \int (-R_s i_{s\alpha-mes} + v_{s\alpha}) dt, \quad (13)$$

$$\Phi_{s\beta} = \int (-R_s i_{s\beta-mes} + v_{s\beta}) dt,$$

The angle θ_s is calculated from:

$$\theta_s = \text{arg}\left(\frac{\Phi_{s\beta}}{\Phi_{s\alpha}}\right) \quad (14)$$

$$T_{em} = p(\Phi_{s\alpha} i_{s\beta} - \Phi_{s\beta} i_{s\alpha}) \quad (15)$$

The estimated values of torque T_{em} and the stator flux Φ_s are respectively compared to reference values T_{em-ref} and Φ_{s-ref} , using two elements non-linear of type hysteresis for knows information of trends evolution of flow and torque. A decision table (table1) enables of determine the states switching as a function the output of each regulator to hysteresis and number of sector θ_i in which is located stator flux vector [1].

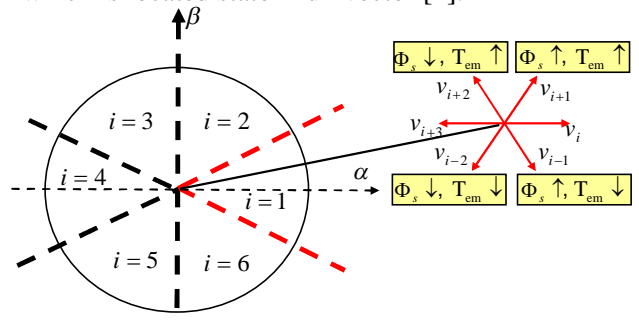


Fig. 6. Selection of voltage vector

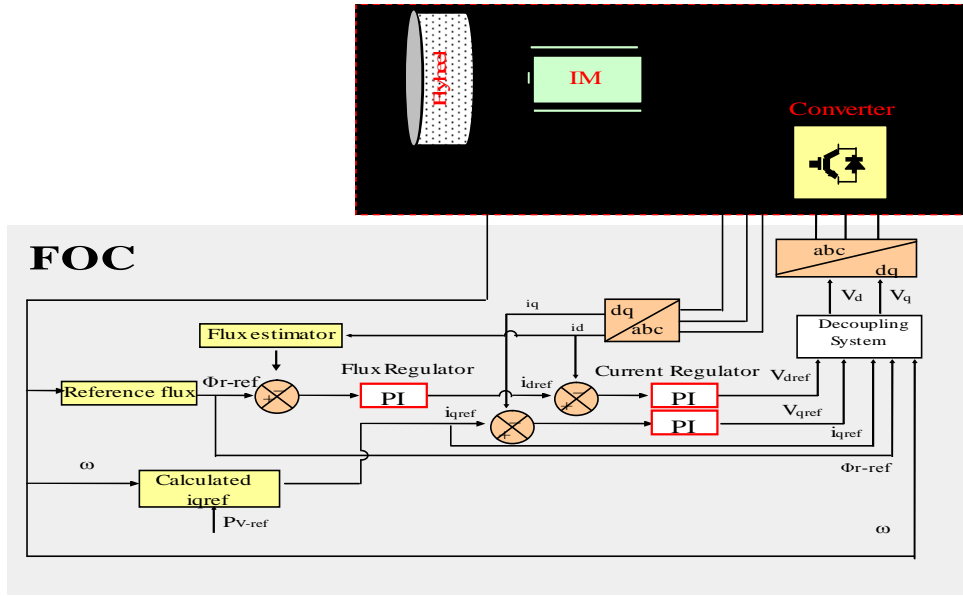


Fig. 3. Block diagram of the control system of inertial storage inertial

Flux	torque	θ_1	θ_2	θ_3	θ_4	θ_5	θ_6
$\uparrow \Phi_s $	$\uparrow T_{em}$	v_2	v_3	v_4	v_5	v_6	v_1
	$\downarrow T_{em}$	v_6	v_1	v_2	v_3	v_4	v_5
$\downarrow \Phi_s $	$\uparrow T_{em}$	v_3	v_4	v_5	v_6	v_1	v_2
	$\downarrow T_{em}$	v_5	v_6	v_1	v_2	v_3	v_4

Table 1. Switching table for DTC control

Fig. 6 shows an example in which the stator flux vector is located in the θ_1 .

If you wish to increase both the flux and torque, this is the vector v_2 which must be applied, because in this sector, among the six active vectors, only the vector v_2 increases the image of the torque and the amplitude of stator flux vector

3. Simulation result

Figures 7, 8, 9 and 10 illustrate the operation of the storage system inertial, with the two control techniques FOC and DTC. The value of the inertia coefficient was calculated for a speed range between 157rad/s and 314rad/s, and a rated power of 1.5kW during a time corresponding to 2.5s.

The initial velocity of the steering wheel is fixed 157rad/s. When the storage reference power P_{v-ref} is set at 1.5kW, the speed increases of 157rad/s to 314rad/s. the system stores energy. When the power is fixed to -1.5kW, the speed decreases of 314rad/s to 157rad/s. The system provides energy as shown in figures 7 and 8.

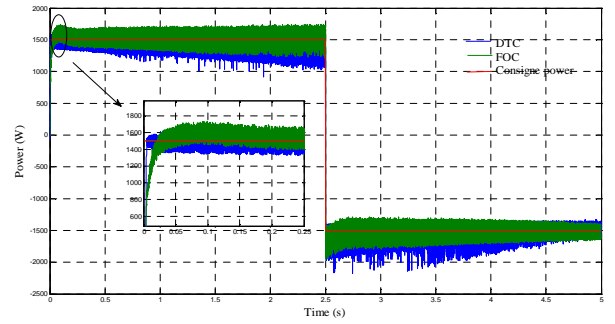


Fig. 7. The power delivered or absorbed by the IM

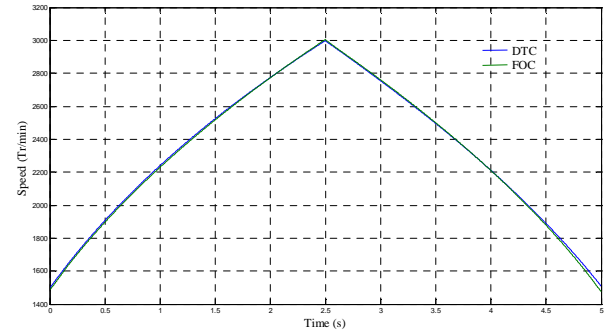


Fig. 8. Speed of the flywheel

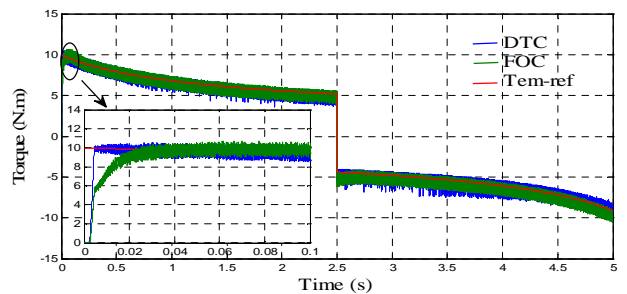


Fig. 9. The electromagnetic torque

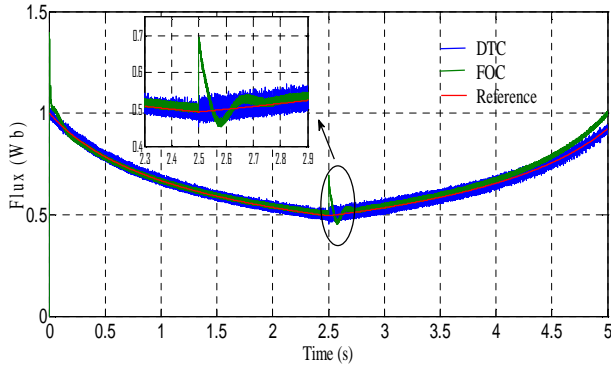


Fig. 10. Modulus stator flux

At level of power and torque (Figures 7 and 9), we notice that the DTC has a high dynamic without overshoot at start-up, and the response time is reduced relative to the FOC. This difference in the transient is due to the presence of PI in control FOC which delay the torque is consequence the power.

Fig. 10 shows the shape of the rotor flux modulus, its reference value is chosen to $\Phi_{rd-ref}=1\text{Wb}$ for both techniques, Field-oriented Control and Direct torque control.

The module response of the rotor flux reaches its reference value without overshoot at startup and is insensitive to variations in the speed of the flywheel for the DTC at time $t=2.5\text{s}$, in effect contrary to the vector control.

Fig. 11 represent the current i_s , the amplitude and the frequency scale due to variation in speed flywheel. Note that the field-oriented control is characterized by low ripples comparing to DTC for different magnitudes: stator current, torque, power and flow.

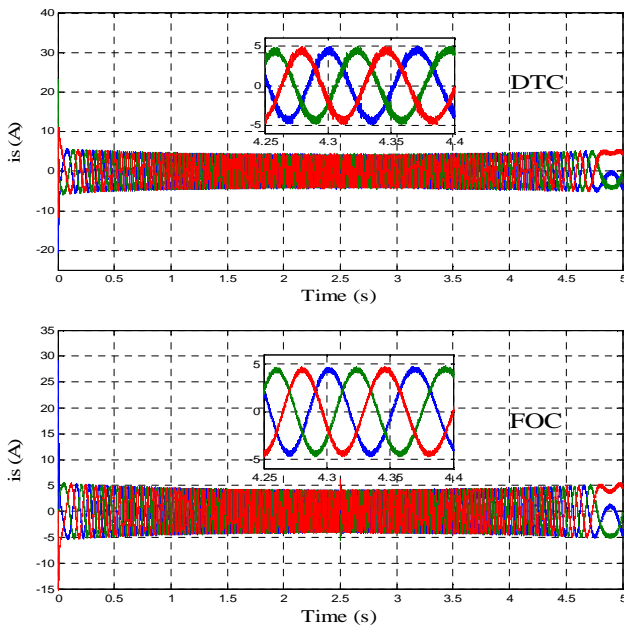


Fig. 11. Stator current

The components of direct and quadrature rotor flux of IM are shown in Fig. 12 for the case FOC. The quadrature component is always zero, which justifies the control in rotor flux oriented.

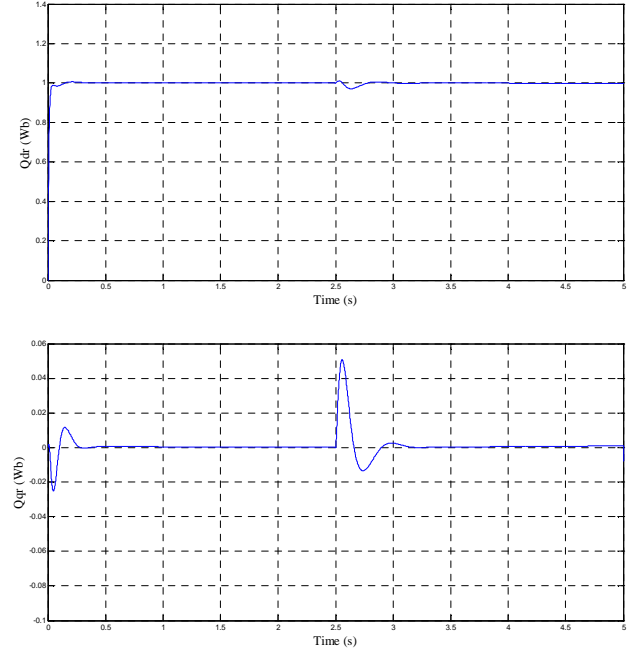


Fig. 12. The flow of direct and quadrature axis

Fig. 13 shows the evolution of two flux components, the modulus of the flow remains close to the reference and is not influenced by variations in the speed of the flywheel (case DTC). Fig. 14 shows the area of work.

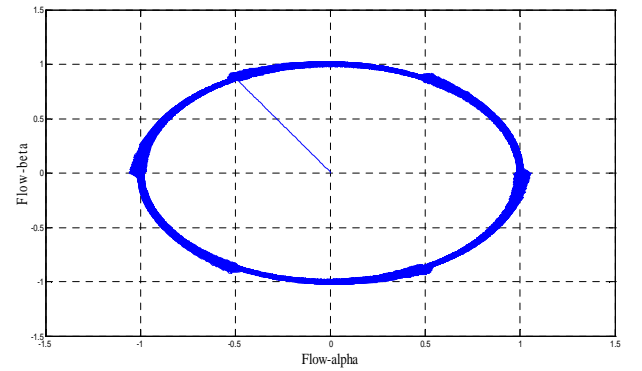


Fig. 13. Stator flux

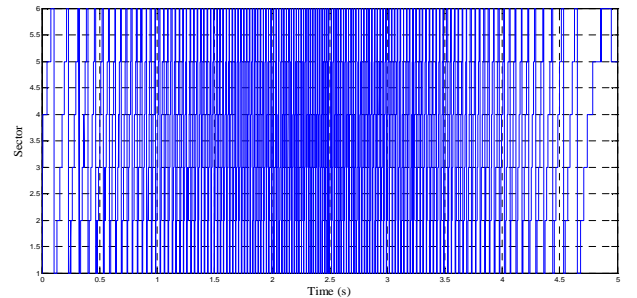


Fig. 14. The variation of the sector

4. Conclusion

In this paper, two control methods are considered for the IM use in an FESS: the field-oriented control (FOC) and direct torque control (DTC). Both control methods give similar performance, with a slight advantage of the FOC control in regime permanent. The use of regulators to hysteresis makes the DTC control little sensitive to variations parametric of the machine. However, they lead to a variable switching frequency in the inverter. This implies a rich harmonic content which increases the losses, leads to acoustic noise and torque oscillations can excite mechanical resonances. In regime dynamic DTC control presents a better response.

The best method will be one that will be improved by modern technology in order to keep the benefits and eliminate the drawbacks.

References

1. Toufouti R., Meziane S., Benalla H.: *Direct torque control for induction motor using fuzzy logic*. ACSE Journal, Vol.6, Issue (2), June, 2006.
2. Bouchafaa F., Hamzaoui I., Boukhalfa S., Talha A.: *Control the Flywheel Storage System by fuzzy logic associated with the wind generator*. (NuRER'2012), Istanbul, Turkey, May 20-23, 2012.
3. Bouhali O., François B., Saudemont C., Berkouk E.M.: *Practical power control design of a NPC multilevel inverter for grid connection of a renewable energy plant based on a FESS and a Wind generator*. IEEE, 2006.
4. Hamzaoui I., Bouchafaa F., Talha A., Boukhalfa A.: *Fuzzy logic control for a speed of a flywheel energy storage system associated the wind Generator*. Acemp-Electromotion 2011, 8-10 Septembre 2011 Istanbul-Turkey.
5. Benaïcha S., Zidani F., Nait Said R., Nait Said M.S.: *Improved DTC of induction motor with fuzzy resistance estimator*. EUSFLAT- LFA 2005.
6. Ouledali O., Meroufel A., Wira P., Nefsi M., Hamouda M.: *Réduction des fluctuations du couple et flux de la commande DTC d'une MSAP par la technique MLI vectorielle*. International Conference on Energy Sustainable Development ICESD'11, 29-30 November 2011, Adrar
7. Ziane H., Retif J.M., Rekioua T.: *Control DTC à fréquence fixe appliqué à une MSAP avec minimisation des oscillations du couple*. Can. J. Elect. Comput. Eng., Vol. 33, No. 3/4, Summer/ Fall 2008.
8. Idjdarene K.: *Contrôle d'une génératrice asynchrone à cage dédiée à la conversion de l'énergie éolienne*. JCGE'08 Lyon, 16-17 Décembre 2008.
9. Toufouti R., Benalla H., Meziane S.: *Contrôle direct du couple de la machine asynchrone alimentée par un onduleur de tension trois- niveaux*.
10. Youb L., Craciunescu A.: *Etude comparative entre la commande vectorielle à flux orienté et la commande directe du couple de la machine asynchrone*. U.P.B. Sci. Bull., Series C, Vol. 69, No. 2, 2007.

Induction machine parameters:

$P=1.5\text{kW}$, $R_s=4.85\Omega$, $R_r=3.805\Omega$, $L_s=L_r=0.274\text{H}$, $L_m=0.258\text{H}$, $p=2$, $J=0.031\text{kg.m}^2$, $f=0.001136\text{N.m.s/rd}$.